SPATIAL HETERODYNE SPECTROSCOPY FOR HIGH SPEED MEASUREMENTS OF STARK SPLIT NEUTRAL BEAM EMISSION IN A HIGH TEMPERATURE PLASMA

by

M.G. BURKE, R.J. FONCK, G.R. MCKEE and G.R. WINZ

28 AUGUST 2018

This is an author-prepared accepted manuscript of M.G. Burke et al., Rev. Sci. Instrum. ***89****, 10D114 (2018), DOI: 10.1063/1.5039285*

ACKNOWLEDGMENT

This material is based upon work supported by the U.S. Department of Energy, Office of Science, Office of Fusion Energy Sciences, under Award Numbers DE-FG02-89ER53296 and FC02-04ER54698.

DISCLAIMER

This report was prepared as an account of work sponsored by an agency of the United States Government. Neither the United States Government nor any agency thereof, nor any of their employees, makes any warranty, express or implied, or assumes any legal liability or responsibility for the accuracy, completeness, or usefulness of any information, apparatus, product, or process disclosed, or represents that its use would not infringe privately owned rights. Reference herein to any specific commercial product, process, or service by trade name, trademark, manufacturer, or otherwise does not necessarily constitute or imply its endorsement, recommendation, or favoring by the United States Government or any agency thereof. The views and opinions of authors expressed herein do not necessarily state or reflect those of the United States Government or any agency thereof.

Spatial heterodyne spectroscopy for high speed measurements of Stark split neutral beam emission in a high temperature plasma

M. G. Burke,[a] R. J. Fonck, G. R. Mckee, and G. R. Winz

Department of Engineering Physics, University of Wisconsin-Madison, Madison, Wisconsin, 53706, USA

(Presented 18 April 2018; received 7 May 2018; accepted 3 July 2018; published online 28 August 2018)

Measurement of electrostatic potential, or local electric field, turbulence is a critical missing component in validating nonlinear turbulence and transport simulations of fusion plasmas. A novel diagnostic is being developed for measuring local electric field fluctuations, $\tilde{E}(r,t)$, via high-speed measurements of the light emitted from a hydrogenic neutral beam. It exploits the proportionality of the spectral line splitting from the Motional Stark Effect to the total electric field experienced by the neutral at the excitation site. The measurement is localized by the usual cross-beam geometry of beam-spectroscopy measurements. The corner stone of the diagnostic is a high spectral resolution, high etendue spatial heterodyne spectrometer (SHS). A SHS design with high etendue (~5 mm^{2}sr) and resolution (~0.14 nm) meets the formidable spectrometer requirements. Field tests of the spectrometer at the DIII-D tokamak demonstrate that the beam emission spectrum produced by the SHS agrees with that of a traditional spectrometer and that the measured flux is adequate for turbulence studies.

I. INTRODUCTION

Resolving the underlying physics of plasma turbulence and the associated cross-field transport of particles, energy, and momentum remains a key scientific challenge facing fusion energy science. Turbulence in tokamaks results in cross-field transport of particles and energy that is typically observed to be two orders of magnitude larger than neoclassical theory predictions. The turbulence manifests as fluctuations in the electron, ion, and impurity densities and temperatures, bulk plasma velocity, and electrostatic potential and magnetic fields. Numerous turbulence diagnostics have been developed to measure $\tilde{n}$, $\tilde{T}_e$, and $\tilde{T}_i$ in fusion grade plasma experiments. However, measurements of plasma electrostatic turbulence ($\tilde{\phi}$) are typically severely limited due to diagnostic availability. For instance, the heavy ion beam[1] probe technique provides electrostatic fluctuations but is logistically complex, while Langmuir probes are typically limited to the colder plasma edge.

Plasma electric field fluctuations ($\tilde{E}_p \sim k_\perp \tilde{\phi}$) crossed with the background magnetic field result in $\vec{E} \times \vec{B}$ velocity fluctuations. These velocity fluctuations are integral to several outstanding tokamak physics topics; however, they are not generally available due to the lack of direct measurements of $\tilde{E}$. For example, the radial velocity fluctuation $\tilde{v}_r \cong \tilde{E}_\theta \times B_\phi$ is required for determining the turbulence-induced cross-field transport. The poloidal velocity $\tilde{v}_\theta \cong \tilde{E}_r \times B_\phi$ is important for flows, and both $\tilde{v}_\theta$ and $\tilde{v}_r$ are important for determining the turbulence-induced Reynolds stress. In addition to providing new insights into current high temperature plasmas, measurements of both these quantities are essential for the validation of gyro-kinetic simulations and plasma turbulence theory.

This paper describes the design and prototype field tests of a novel diagnostic to directly measure $\tilde{E}_p$ in a high temperature magnetized plasma. The approach employs elements of techniques used in Motional Stark Effect (MSE) measurements,[2] beam emission spectroscopy,[3,4] and high-speed ion temperature measurements in tokamaks.[5] The premise of the diagnostic is to spectrally resolve the hydrogenic beam emission (orthogonally polarized π and σ components) at speeds relevant to turbulence. The spectral separation of these components ($\Delta\lambda$) is linearly proportional to the magnitude of the electric field in the inertial frame of the neutral atom as it traverses the magnetized plasma. The total electric field experienced by the neutral is the superposition of the MSE ($\vec{E}_{MSE}$) and plasma (also referred to as intrinsic) electric fields ($\vec{E}_p$). Therefore, fluctuations in the intrinsic electric field of the plasma will result in small changes in the spectral separation of the beam emission components. The magnitude of plasma electric field fluctuations is small. Based on simple scaling relations for drift-wave turbulence and previous measurements,[6] $|\tilde{E}_p|/|\vec{E}_{MSE}| \sim 10^{-3}$ when normalized to the MSE field magnitude. The resulting fluctuations in the spectral separation of the two groups of π components compared to the nominally static separation from $\vec{E}_{MSE}$ are similarly small, $\tilde{\Delta\lambda}_{\tilde{E}}/\Delta\lambda_{\vec{E}_{MSE}} \sim 10^{-3}$.

Measurements of such small spectral shifts with sufficient etendue to detect fluctuations above inherent photon noise are possible using the Spatial Heterodyne Spectroscopy (SHS) interferometric technique. This technique achieves the interferometric luminosity-resolution advantage over dispersive systems. Therefore, the etendue of a SHS is typically several orders of

Note: Paper published as part of the Proceedings of the 22nd Topical Conference on High-Temperature Plasma Diagnostics, San Diego, California, April 2018.

[a]Author to whom correspondence should be addressed: mgburke@wisc.edu.

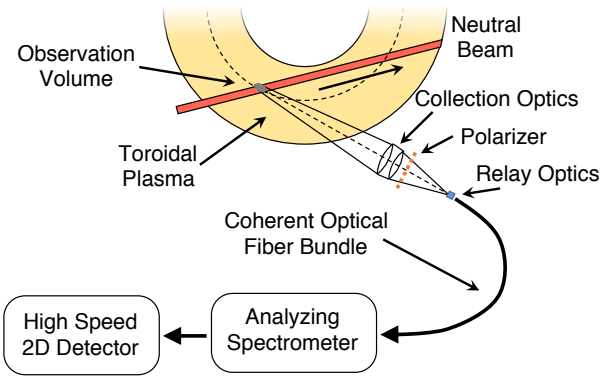

FIG. 1. Schematic of the layout of the $\tilde{E}$ diagnostic.

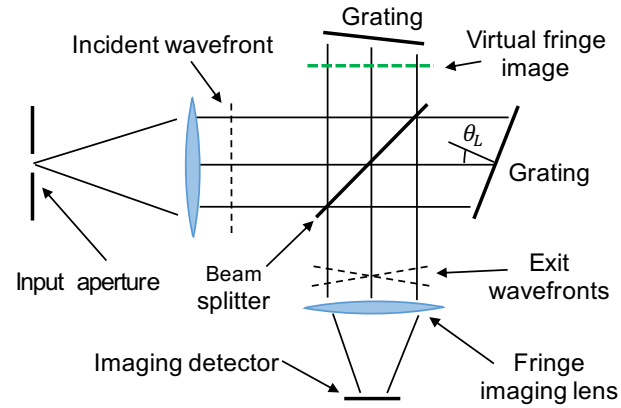

FIG. 2. Conceptual drawing of the spatial heterodyne spectroscopy technique.

magnitude larger than standard dispersion spectrometers of similar size and spectral resolution. This makes SHS well suited for turbulence spectroscopy.

This paper presents the design and testing of a prototype SHS spectrometer purpose built for the evaluation of the $\tilde{\Delta}\lambda_{\tilde{E}}(t)$ measurement. Slow timescale spectra from a field test of the spectrometer at the DIII-D tokamak are used to evaluate compatibility with a tokamak environment. A Doppler-compensating spectrometer concept, similar to that used in planetary atmospheric spectroscopy, is employed to support the very high etendue optics necessary for turbulence diagnostics.

II. DIAGNOSTIC PRINCIPLES

The basic approach of the diagnostic is to spectrally resolve the Motional Stark Effect (MSE) split neutral beam emission of the D_α ($n = 3 \rightarrow 2$, $\lambda_0 = 656.1$ nm) line. The wavelength separation between adjacent components of the Stark spectrum is linear in $|\vec{E}|$ (for $|\vec{E}| \lesssim 10$ MV/m) and is determined by atomic physics to be $\Delta\lambda_{\sigma,\pi} \cong 0.027|\vec{E}|n$, where $|\vec{E}|$ is in MV/m, $\Delta\lambda$ is in nm, and n is the state transition number ($n = 0, \pm1$ for σ and $n = \pm2, \pm3, \pm4$ for π). With sufficient neutral beam velocity and an appropriate viewing geometry, measurement of fast changes in the spectral separation of the Stark components, $\Delta\lambda_{\sigma,\pi}(t)$, will provide measurements of the fluctuations in $\vec{E}_p$, assuming for the moment that the other contributions (such as changes in neutral beam velocity or the plasma magnetic field) are small.

This work focuses on the measurement of fluctuations in the overall spectral separation of only the π components of the Stark multiplet using a midplane sightline. The removal of the σ components reduces the resolution requirements of the spectrometer by isolating the spectrum to the components with the highest $\Delta\lambda$ for a given $|E|$. Note that this sight line is sensitive to poloidal fluctuations ($\tilde{E}_\theta$) only because $\vec{E}_{MSE} \gg \vec{E}_p \approx \vec{E}_r + \vec{E}_\theta$ and $\vec{E}_\theta$ is in nominally the same direction as $\vec{E}_{MSE}$. This greatly suppresses the contribution of radial fluctuations ($\tilde{E}_r$) to $|E_t|$. Of course, additional sightline geometries can provide access to $\tilde{E}_r$ as needed.

III. PROTOTYPE DIAGNOSTIC DESIGN

The basic layout of the midplane-viewing diagnostic is shown in figure 1. The layout consists of 6 major components: (1) a large diameter plasma collection lens to image a small volume of plasma (typical spatial scale ~ 1 cm) to an optical fiber bundle; (2) a linear polarizer to isolate the MSE components of interest; (3) a set of relay lenses to form an image of the collection lens at the fiber bundle while maintaining the plasma spatial resolution (necessary for the correction of geometric Doppler broadening); (4) a coherent fiber bundle; (5) a high etendue and resolution analyzing spectrometer; and finally (6) a high speed imaging detector system.

Parameters of the DIII-D tokamak plasma, neutral beams, and available high etendue optical system parameters inform major design points of the prototype spectrometer. The existing DIII-D BES collection optic system[7] (~20 cm diameter lens, f/3 imaging) is coupled to a new small compound relay lens system (~4 mm diameter, 5.8 mm effective focal length) to collect light from the plasma (~1 cm plasma spatial resolution). The light is carried to the analyzing spectrometer via a single fiber bundle (seven 1 mm diameter fibers in a 2:3:2 arrangement). A linear polarizer is installed immediately in front of the bundle to remove the σ components of the beam emission. Only the π components are transmitted to the spectrometer.

A. Spatial Heterodyne Spectroscopy

The SHS technique was chosen for the analyzing spectrograph for its high resolution and optical etendue capabilities.[8,9] SHS is a method of Fourier transform spectroscopy based on a Michelson interferometer in which the two mirrors are replaced by gratings.

The basic layout of a SHS spectrometer is shown in Fig. 2. The gratings create a wavelength-dependent crossing angle between the recombined wavefronts that exit the interferometer. The interference of these wavefronts results in a Fizeau fringe pattern (interferogram) that is composed of wavelength dependent spatial frequencies that are heterodyned around the Littrow wavelength of the gratings.

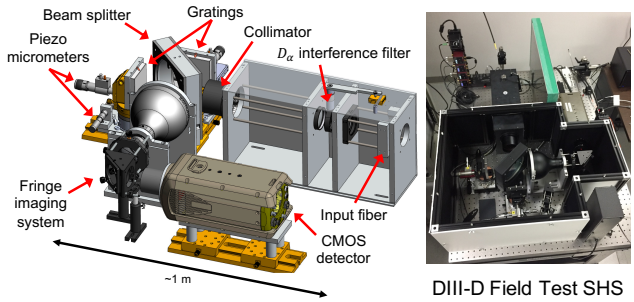

FIG. 3. Schematic and photograph of the prototype SHS built for field tests at the DIII-D tokamak.

This is described by the output interferogram equation for the SHS,

$$I(x) = \int d\sigma\, B(\sigma)\left[1 + \cos\left(2\pi(4(\sigma - \sigma_L)x \tan\theta_L)\right)\right], \quad (1)$$

were $B(\sigma)$ is the input spectrum, $I(x)$ is the intensity across the detector plane, and θ_L and σ_L are the Littrow angle and wavenumber, respectively. The virtual image of the fringes is localized near the grating faces and is imaged to a detector by the exit optics.

B. Design Points of SHS for $\Delta\lambda_\pi(t)$

A prototype SHS spectrometer was built and its performance characterized at the University of Wisconsin–Madison before being deployed for field tests on the DIII-D tokamak. Off-the-shelf components were used as much as possible to minimize costs and maximize the flexibility of the system.

The etendue and spectral resolution requirements of the spectrometer are defined as follows. The etendue of the spectrometer must match the collection optics etendue ($U = A\Omega$, where A is the area and Ω is the solid angle of the source through the limiting aperture). The etendue of a single DIII-D BES channel (single spatial point in the plasma) is $U =$ 1.6 mm^2 sr.

The spectral resolution required is set by the number of spectral bins needed to resolve small changes in the separation of the π components. The number of spectral bins is based on past experience with the $\tilde{T}_i$ diagnostic.[5,10] This work showed that 4 spectral bins could resolve changes to the distribution centroid to a small fraction (~0.1%) of the distribution width. Therefore, a minimum number of 8 spectral channels are needed to resolve changes in the separation of the two approximately Gaussian π component sets of the full beam energy Stark multiplet. For typical DIII-D operations (B_{T0} ~ 2 T and 75 keV deuterium beam) these components span ~1 nm, thus the resolution required is $\delta\lambda \lesssim 0.125$ nm.

The spectral resolving power, $R = \lambda/\delta\lambda$, of the SHS is $R = 4W\sigma \sin\theta_L$, where W is the grating width, σ is the wavenumber, and θ_L is the Littrow angle. The gratings chosen for this prototype design work were off-the-shelf 7.62 cm square gratings with a groove density of 50 g/mm. This gives a resolving power of 7620 and a resolution $\delta\lambda =$ 0.086 nm ($\delta\sigma = 2$ cm^{-1}) at 656 nm.

The maximum field-of-view of the SHS, Ω_m, is limited by the resolving power to $\Omega_m = 2\pi/R$. This gives a maximum etendue for the spectrometer of 4.8 mm^2 sr. The excess etendue allows for future upgrades to multiple plasma spatial points through a single spectrometer.

A schematic and photograph of the prototype SHS spectrometer are shown in Fig. 3 with the major components highlighted. Light from the plasma is directed into the SHS by one of the DIII-D BES fiber bundles. The fiber 2:3:2 cross-section acts as the input aperture for the spectrometer. A prefilter system consisting of two 100 mm focal length f/2 achromats, image the output of the fiber through a high transmission efficiency (>90%) interference filter. The filter 0° angle of incidence central wavelength is 654 nm and it has a 90% bandwidth of ~2.4 nm. The 90%-10% transmission cutoff of the filter is designed to be ~0.25 nm. This allows for measurements of only the full beam energy components if desired.

The output of the filter is then collimated through a 150 mm focal length f/2 achromat. A ~152 mm diameter 50:50 non-polarizing beam splitter plate with $\lambda/4$ flatness and a matching compensator plate split the beam towards the two gratings. The fringe pattern, which is virtually located close to the surface of the gratings, is imaged by a telecentric lens with a magnification of 0.28 and a depth-of-field of 8 mm. The output image of the telecentric is further reduced using a 25 mm focal length f/0.95 compound lens and field lens to a final image size of ~2.5 mm diameter at the detector. The detector used for the DIII-D field tests was a Phantom v310 from Vision Research.

C. Laboratory Characterization

Figure 4(a) shows a typical fringe pattern that is generated by the spectrometer when viewing a monochromatic source (Hydrogen 656 nm line). The fringe contrast with the 4.5 mm aperture diameter (necessary to fit the fiber bundle) is ~90% compared to 95% for the 1 mm aperture. This indicates that the loss-of-contrast due to the increase in the spectrometer field-of-view and contamination from stray light is acceptable.

Figure 4(b) shows the magnitude of a Fourier transform of the 4.5 mm aperture monochromatic interferogram shown in Fig. 4(a) after flat field correction, zero padding, and apodization with a Hanning window function. The spectrum displays the characteristic sinc-like instrumental function. For Fourier transform spectroscopy, the spectral resolution is defined as the half-width of the sinc instrumental function at the first zeros. Taking these values from Fig. 4(b), this gives a resolution of $\delta\sigma \approx 3.3$ cm^{-1} ($\delta\lambda \approx 0.14$ nm). The measured resolution is expected to be ~2× larger than the theoretical value due to the Hanning window function.

The spectrometer was photometrically calibrated in the lab to evaluate the spectrometer photon detection efficiency.

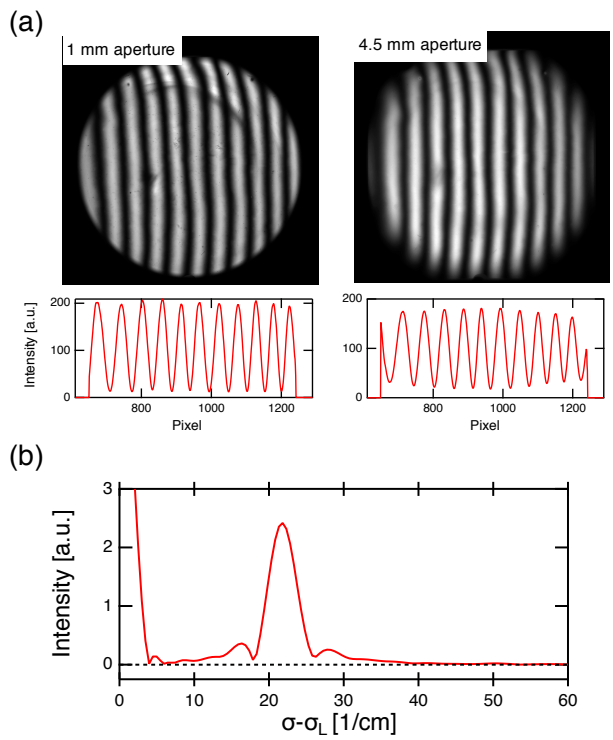

FIG. 4. (a) SHS fringe image and horizontal cut through generated by monochromatic source (H_α, 656 nm) through 1 mm (left) and 4.5 mm (right) aperture. (b) FFT of 4.5 mm aperture interferogram.

This was measured from the input aperture to the detector to be ~8%. This roughly agrees with the product of the manufacturer specified component and overall system efficiencies, consisting of the gratings (~70%), detector efficiency (~30%), 2-beam 50% loss, fringe imaging and prefilter system of 5 compound lenses (~93%), and interference filter (95%) giving a total of ~9%.

IV. FIELD TEST ON DIII-D

A field test of the prototype spectrometer on the DIII-D tokamak was performed in order to evaluate the signal level achievable and its viability for turbulence measurements as well as to evaluate the spectrometer's susceptibility to environmental conditions (vibrations, temperature swings, radiation, etc.).

Beam emission spectra taken from the SHS and a traditional spectrometer agree qualitatively, indicating that the SHS is working as expected. The top panel of Fig. 5 shows a comparison of the beam emission for DIII-D plasma shot 175827 as measured by a 1/2 m Czerny-Turner spectrometer (100 μm slit width, 2400 g/mm, $\delta\lambda \approx 0.05$ nm) and the SHS described above. A linear polarizer removes the σ components of the spectrum and therefore only the π components of the different beam energy species are recorded. The bottom two panels in Fig. 5 show the raw fringe image and the fringe intensity from a horizontal cut of the image. The integration time for the SHS image was 10 ms (250 ms for the 1/2 m) and the deuterium neutral beam energy was 58 keV.

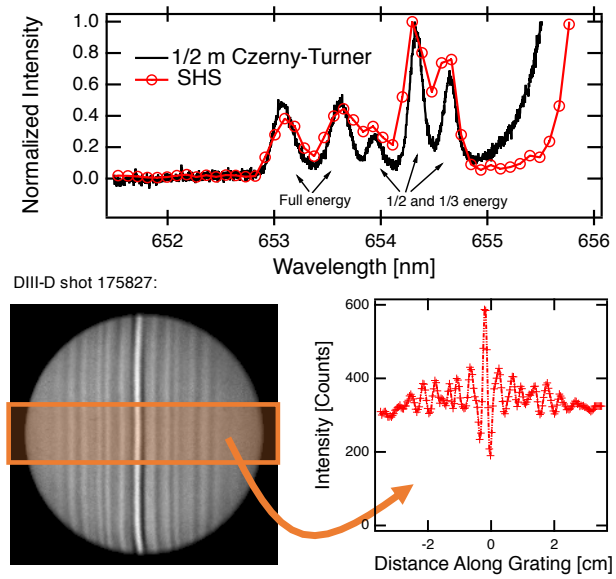

FIG. 5. Top: Comparison of beam emission spectrum recorded by 1/2 m Czerny-Turner spectrometer and SHS. Bottom: Raw SHS fringe image and the cut through plot showing the corrected interferogram used to produce the SHS spectrum.

The total signal level of the π components measured in Fig. 5 is 3-4 $\times 10^9$ photons/s. This gives ~1.5% photon noise statistics at a bandwidth of 500 kHz. This is comparable to the typical BES photon noise level of ~1% and should be adequate to begin turbulence studies.

In addition to the basic validation studies described above, the field test provided valuable experience with the spectrometer in other areas. For instance, further suppression of environmental vibrations is needed to remove a small ($\sim\lambda/10$ differential change in the zero-path length difference) lateral movement of the fringe pattern at ~60 Hz (likely from nearby HVAC equipment). In addition, closed loop piezo micrometers and a *in situ* calibration source were installed so that gradual misalignment of the interferometer due to temperature changes and/or vibrations could be fixed remotely.

V. CORRECTION OF GEOMETRIC DOPPLER BROADENING IN SHS

The individual Stark components are spectrally broadened by several effects inherent to the measurement. These effects include the neutral beam ion source temperature, divergence in neutral beam ion optics, and geometric Doppler broadening due to the high etendue plasma collection lens.

Geometric Doppler broadening is the dominant broadening mechanism in this measurement and thereby limits the diagnostic's sensitivity to $\tilde{E}$. The broadening is due to optical rays horizontally displaced across the collection lens intersecting the neutral beam at different angles. Adjacent sections therefore have different Doppler shifts, resulting in a net broadening of the observed spectrum. The amount of spectral shift across the lens

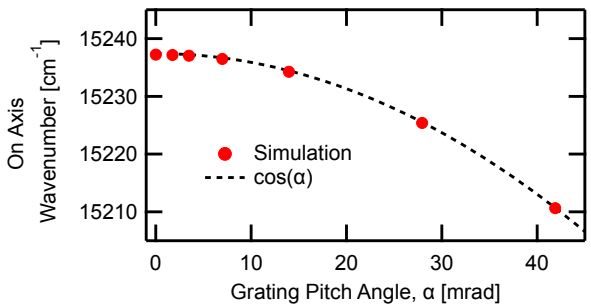

FIG. 6. Simulation of the effective input wavenumber of the SHS with increasing grating pitch angle.

aperture can be large. For typical DIII-D parameters, the amount of geometric broadening is ~0.5 nm, while spectral fluctuations from $\tilde{E}_p$ are ~0.1% of that.

Compensation of the geometric Doppler shift is possible inside the SHS using techniques similar to those employed in planetary atmospheric and atomic beam interferometry.[11,12] In these systems, the Doppler shift due to planetary rotation or source velocity is compensated for by imposing an equal but opposite shift in the wavenumber passband across the entrance aperture that matches the Doppler shift across the planetary image or collection lens. The shift in the passband is imposed by tilting the interferometer off-axis.

For the SHS technique, this compensation can be accomplished in a similar manner: by mapping the known linear wavelength shift across the collection optic to an off-axis angle at the face of each grating. In practice, this is accomplished by placing an image of the collection lens at the SHS input aperture and then either tilting the gratings or moving the input aperture off the optical midplane by an angle α. The $\cos\alpha$ dependence of the grating dispersion means that different field angle points across the aperture experience a different effective groove density. If correctly tuned, the different field angle wavelengths will exit at the same angle. Thus the net interferogram spatial frequency can be kept constant even though the input wavenumber is changing across the aperture.

Ray tracing analyses of a tilted SHS qualitatively demonstrates the geometric broadening compensation concept in SHS. Here, a SHS with monochromatic input (λ_{in} = 656 nm, 50 g/mm, θ_L= 0.0164 rad) was modeled and the spatial frequency at varying grating tilt angles was measured. An effective input wavenumber was then calculated using Eq. (1). Figure 6 plots the measured effective input wavenumber vs grating pitch angle α. The simulation confirms the dependence of the effective input wavenumber with $\cos\alpha$ (black dashed line). In practice, the tilt angle of the grating must be matched to a given linear wavenumber shift across the input aperture ($\delta\sigma/\delta\alpha$).

VI. CONCLUSION

A prototype SHS spectrometer with high etendue and resolution has been developed to meet the formidable spectrometer requirements for measuring high speed fluctuations of the deuterium MSE spectrum. Spectra produced by the prototype spectrometer in the laboratory and field tests on the DIII-D tokamak demonstrate the spectrometer is working as expected. These tests also indicate that the photon flux is adequate for turbulence studies. Future work includes increasing the spectrometer resilience to vibrations and deploying a high-speed imaging detector system.

ACKOWLEDGMENTS

The authors thank D. Truong for his assistance with the spectrometer work. This material is based upon work supported by the U.S. Department of Energy, Office of Science, Office of Fusion Energy Sciences, under Award Nos. DE-FG02-89ER53296 and FC02-04ER54698.

Data from this publication are publicly available in openly-documented, machine-readable formats and are available at https://doi.org/10.18138/1435641.

This report was prepared as an account of work sponsored by an agency of the United States Government. Neither the United States Government nor any agency thereof, nor any of their employees, makes any warranty, express or implied, or assumes any legal liability or responsibility for the accuracy, completeness, or usefulness of any information, apparatus, product, or process disclosed, or represents that its use would not infringe privately owned rights. Reference herein to any specific commercial product, process, or service by trade name, trademark, manufacturer, or otherwise, does not necessarily constitute or imply its endorsement, recommendation, or favouring by the United States Government or any agency thereof. The views and opinions of authors expressed herein do not necessarily state or reflect those of the United States Government or any agency thereof.

[1] G.A. Hallock *et al.*, Phys. Rev. Lett. **56**, 1248 (1986).
[2] F.M. Levinton *et al.*, Phys. Rev. Lett. **63**, 2060 (1989).
[3] R.J. Fonck *et al.*, Rev. Sci. Instrum. **61**, 3487 (1990).
[4] R.D. Durst *et al.*, Rev. Sci. Instrum. **63**, 4907 (1992).
[5] H.T. Evensen *et al.*, Nucl. Fusion **38**, 237 (1998).
[6] C.P. Ritz *et al.*, Phys. Rev. Lett. **62**, 1844 (1989).
[7] G.R. McKee *et al.*, Rev. Sci. Instrum. **70**, 913 (1999).
[8] J. Harlander *et al.*, Astrophys. J. **396**, 730 (1992).
[9] C.R. Englert *et al.*, Appl. Opt. **54**, F158 (2015).
[10] G.R. McKee *et al.*, Rev. Sci. Instrum. **79**, 10F528 (2008).
[11] J.T. Trauger and F.L. Roesler, Appl. Opt. **11**, 1964 (1972).
[12] F.L. Roesler and J.O. Stoner Jr., Nucl. Instrum. Methods **110**, 465 (1973).